Decadal morphological evolution of the mouth zone of the Yangtze Estuary in response to human interventions

Zhu, Chunyan; Guo, Leicheng; van Maren, Bas; Tian, Bo; Wang, Xianye; He, Qing; Wang, Zheng Bing

DOI
10.1002/esp.4647

Publication date
2019

Document Version
Final published version

Published in
Earth Surface Processes and Landforms

Citation (APA)
Zhu, C., Guo, L., van Maren, B., Tian, B., Wang, X., He, Q., & Wang, Z. B. (2019). Decadal morphological evolution of the mouth zone of the Yangtze Estuary in response to human interventions. *Earth Surface Processes and Landforms*, *44*(12), 2319-2332. https://doi.org/10.1002/esp.4647

EARTH SURFACE PROCESSES AND LANDFORMS
Earth Surf. Process. Landforms **44**, 2319–2332 (2019)

Published online 18 June 2019 in Wiley Online Library
(wileyonlinelibrary.com) DOI: 10.1002/esp.4647

Decadal morphological evolution of the mouth zone of the Yangtze Estuary in response to human interventions

Chunyan Zhu,[1,2] Leicheng Guo,[1]* Dirk Sebastiaan van Maren,[2,3] Bo Tian,[1] Xianye Wang,[1] Qing He[1] and Zheng Bing Wang[1,2,3]
[1] State Key Laboratory of Estuarine and Coastal Research, East China Normal University, Shanghai 200241, China
[2] Faculty of Civil Engineering and Geosciences, Delft University of Technology, Delft, The Netherlands
[3] Deltares, Delft, The Netherlands

Received 13 July 2018; Revised 24 April 2019; Accepted 2 May 2019

*Correspondence to: Leicheng Guo, State Key Laboratory of Estuarine and Coastal Research, East China Normal University, Shanghai 200241, China.
E-mail: lcguo@sklec.ecnu.edu.cn

ESPL
Earth Surface Processes and Landforms

ABSTRACT: The morphology of the Yangtze Estuary has changed substantially at decadal time scales in response to natural processes, local human interference and reduced sediment supply. Due to its high sediment load, the morphodynamic response time of the estuary is short, providing a valuable semi-natural system to evaluate large-scale estuarine morphodynamic responses to interference. Previous studies primarily addressed local morphologic changes within the estuary, but since an overall sediment balance is missing, it remains unclear whether the estuary as a whole has shifted from sedimentation to erosion in response to reduced riverine sediment supply (e.g. resulting from construction of the Three Gorges Dam). In this paper we examine the morphological changes of two large shoals in the mouth zone (i.e. the Hengsha flat and the Jiuduan shoal) using bathymetric data collected between 1953 and 2016 and a series of satellite images. We observe that the two shoals accreted at different rates before 2010 but reverted to erosion thereafter. Human activities such as dredging and dumping contribute to erosion, masking the impacts of sediment source reduction. The effects of local human intervention (such as the construction of a navigation channel) are instantaneous and are likely to have already resulted in new dynamic equilibrium conditions. The morphodynamic response time of the mouth zone to riverine sediment decrease is further suggested to be >30 years (starting from the mid-1980s). Accounting for the different adaptation time scales of various human activities is essential when interpreting morphodynamic changes in large-scale estuaries and deltas. © 2019 John Wiley & Sons, Ltd.

KEYWORDS: Yangtze Estuary; morphology; human activities; channel–shoal system; response time

Introduction

Many river deltas are densely populated and connected to the sea by tidal channels, which are progressively deepened to provide access to increasingly larger vessels. Sustainable management of such systems (maintaining ecological and recreational functions while allowing economic development) requires in-depth understanding of estuarine and deltaic morphological changes, especially in view of projected sea-level rise. Riverine sediment supply plays an important role in controlling the morphological evolution of many estuaries. The suspended sediment load of rivers has declined globally due to dam construction and soil conservation (Vörösmarty *et al.*, 2003; Syvitski and Saito, 2007; Walling, 2009). Simultaneously, local engineering works (e.g. construction of training walls and jetties; dredging and dumping activities) influence channel and shoal morphology (Sherwood *et al.*, 1990; Thomas *et al.*, 2002; Lane, 2004; Blott *et al.*, 2006; De Vriend *et al.*, 2011; Wang *et al.*, 2015). Since many of these human activities take place concurrently, isolating the morphodynamic impacts of individual human interventions (including sediment supply reduction) from natural morphological evolution is challenging.

The Yangtze Estuary (YE) in China is a large-scale alluvial system whose morphology is influenced by a significant reduction in sediment supply and extensive local human activities. River-borne sediment discharges initially decreased gradually from the mid-1980s but accelerated to the present-day amount of ~70% due to the Three Gorges Dam (constructed in 2003; Yang *et al.*, 2015; Luan *et al.*, 2016; Zhao *et al.*, 2018). Fine sands and silts are mainly trapped in the upstream reservoirs, whereas clay particles are flushed downstream (van Maren *et al.*, 2013). Such a reduced sediment supply is expected to decrease deposition rates and possibly even lead to erosion along the sand-dominated riverbed and in the silt-dominated estuary. Previous work (Table S1 and Figure S1) suggests that the inner estuary has indeed eroded in the past decade. The inner estuary includes the South Branch, South Channel and North Channel (Figure 1), and is mainly controlled by upstream river and sediment discharge (e.g. Luan *et al.*, 2016; Zhao *et al.*, 2018). Erosion has also been observed in the subaqueous delta (e.g. Yang

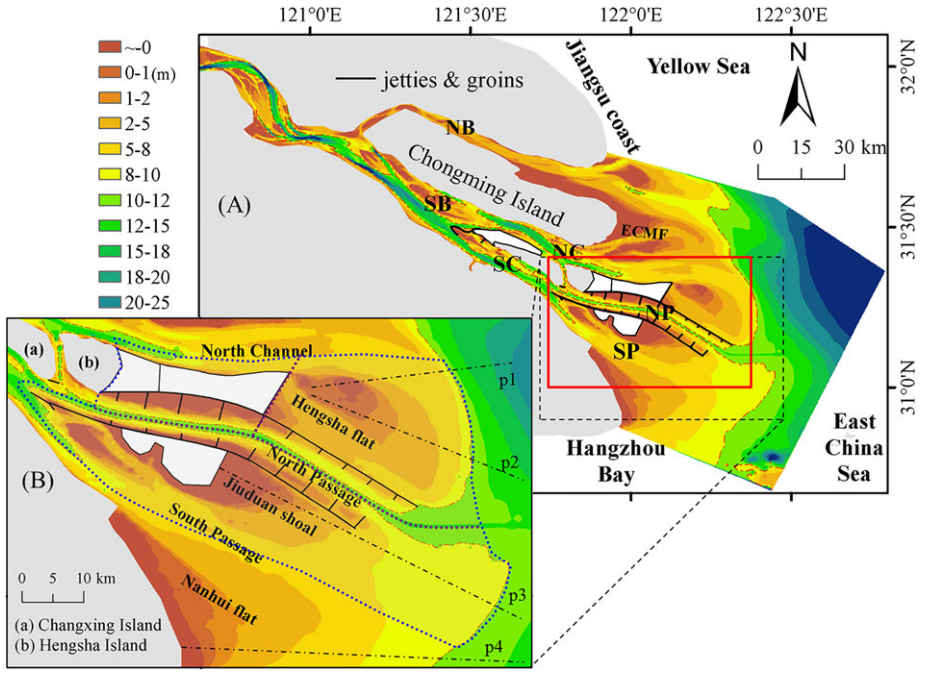

Figure 1. (A) Map of the Yangtze Estuary with the bathymetry in 2013 referencing the TLWL and (B) details of the area of interest, including the Hengsha flat and Jiuduan shoal. The white areas are the reclaimed regions in the landward part of the Hengsha flat and the vegetated supertidal flats of the Jiuduan shoal. NB, SB, NC, SC, NP and SP indicate the North Branch, South Branch, North Channel, South Channel, North Passage and South Passage, respectively. ECMF indicates the eastern Chongming flat, which is located to the east of Chongming Island. The red box in (A) indicates the area used to estimate sand volumes and hypsometry. TLWL: theoretical lowest water level. [Colour figure can be viewed at wileyonlinelibrary.com]

et al., 2003, 2011, 2018). In contrast, investigating a larger part of the subaqueous delta, Dai *et al.* (2014) conclude that the delta was still depositional (at least until 2009). This discrepancy probably results from the definition of the study area: Yang *et al.* (2011) investigated the delta front (depths from 5 to 10 to 15–30 m) and prodelta (depths > 15–30 m), whereas Dai *et al.* (2014) also included the delta plain (depths < 5–10 m), which lies in the mouth zone. The mouth zone is a region under combined river and tidal forcing, where accretion continued for a long time (Wang *et al.*, 2013; Luan *et al.*, 2016; Zhao *et al.*, 2018). Interestingly, erosion of the mouth zone has been detected very recently (Zhao *et al.*, 2018), suggesting that the subaqueous delta as a whole may indeed revert to erosion. These studies highlight the need for further study of the mouth zone, where the morphological response time may be much longer than those in the inner estuary and subaqueous delta.

At a smaller spatial scale, the shoals and tidal flats in the mouth zone are accreting, including the eastern Chongming flat (Yang *et al.*, 2008), Nanhui shoal (Fan *et al.*, 2017; Wei *et al.*, 2017), Jiuduan shoal (Gao *et al.*, 2010; Wei *et al.*, 2015; Li *et al.*, 2016) and Hengsha flat (Wei *et al.*, 2015). Although the accretion rates of some shoals and tidal flats typically decrease (Yang *et al.*, 2008; Wei *et al.*, 2015), erosion has not yet been observed. As a result, it remains unclear whether the mouth zone is presently eroding or deposition still prevails.

Additionally, the mechanisms controlling bathymetric evolution remain unclear. Erosion in the subaqueous delta has been attributed to a reduction in riverine sediment supply (Yang *et al.*, 2003, 2011). In addition, the subaqueous delta of the YE has a transition from the gentle delta plain to the steep delta front at depths of 12–15 m, which is called a rollover point (Hori *et al.*, 2002; Eidam *et al.*, 2017). Such a rollover depth, along with waves, may also contribute to subaqueous erosion, resulting in coarsening of sediment in the subaqueous delta (Luo *et al.*, 2017; Yang *et al.*, 2018).

Local human activities additionally drive morphological changes in the YE (see e.g. Wang *et al.*, 2015). A major intervention was engineering work in the North Passage (NP), involving the construction of a nearly 50 km-long double training wall with groins (see Figure 1). The jetties and groins in the NP are so large that they may induce severe erosion in the mouth of the NP and in the region to the east of Hengsha flat (Zhu *et al.*, 2016). The jetties partially block regional horizontal circulation (Zhu *et al.*, 2016), possibly leading to sediment deposition and accretion over the surrounding flats. In addition, intense dredging and dumping activities take place in the NP. Despite the large dredging effort (~70 million m^3 $year^{-1}$; Wang *et al.*, 2015), this sediment mass is not accounted for in previous estimates of the estuarine sediment balance.

Overall, it therefore remains unclear (1) whether the mouth zone of the YE is still accreting or has become erosive and (2) what the impacts of local human interventions and reduced sediment supply are and at what time scales they operate in. We perform an in-depth analysis of bathymetric changes in the mouth zone using all high-quality bed-level data available (covering a period of ~60 years until 2016) and relate these observations to changes in sediment supply, regional engineering works and salt marsh growth. The eastern Chongming flat, which lacks data in its northern part (see Figure S2) and has a long history of reclamation (since the early 1960s), is omitted from this study. Our study area includes the Hengsha flat, the Jiuduan shoal and the NP landward of the 10-m isobaths in 1997, constituting a total area of approximately 1740 km^2 (Figure 1). The data, including bathymetric maps (1953–2016), are used to provide an overview of the erosion and deposition patterns as well as the long-term hypsometry changes. Satellite images (1985–2016) are employed to study the evolution of the tidal flats and the interactions between morphology and vegetation.

Data and Methods

Study area

The Yangtze River is one of the largest rivers in the world in terms of its length (~6300 km) and catchment area (~1.9 million

km^2). The Datong station, ~640 km landward of the river mouth, is the tidal wave limit in the dry seasons. Here, the mean river discharge is 28 200 m^3 s^{-1}, and the annual suspended sediment load is 364 million tons per year from 1951 to 2016. The river-supplied sediment has stimulated rapid infilling of the pre-incised river valley and build-up of the delta since the mid-Holocene (~7500 years ago). In the past 60 years, the river discharge at Datong has remained stable, whereas the suspended sediment load has gradually decreased since the mid-1980s (Guo *et al.*, 2018) (Figure 2). The decrease in suspended sediment loads is mainly due to soil conservation strategies and dam construction (e.g. Yang *et al.*, 2015). Suspended sediment load reduction is more dramatic (~70%) since 2003, when the Three Gorges Dam (TGD) began operation (Figure 2). Since then, erosion has been detected in the 1200-km river reach between Yichang (approximately 40 km downstream of TGD) and Datong (resulting in a downstream increase in suspended sediment load; see Figure 2). On decadal time scales, the sedimentation rate (1–3 cm year^{-1}; Jia *et al.*, 2018) in the study area is an order of magnitude larger than the rate of sea-level rise in the recent century (3 mm year^{-1} from 1980 to 2015; SOA, 2015).

At its seaward side, the YE is forced by tides with a mean range of 2.7 m and a maximum spring tidal range of 5.5 m (Yun, 2004). Wave energy is moderate at the mouth with a mean wave height of 0.9 m, although wave heights can reach 6.2 m during storm conditions (Yang *et al.*, 2001). Under combined river and tidal forcing, the mouth zone of the YE is a partially mixed environment with strong density currents and lateral circulations due to water exchange between different branches (Wu *et al.*, 2010; Zhu *et al.*, 2018). These lateral circulations, however, are presently decreasing because of elevated tidal flats and the blocking effects of the jetties discussed in the next paragraphs (Zhu *et al.*, 2018).

Morphologically, the YE maintains a configuration with four outlets [i.e. the North Branch, North Channel, NP and South Passage (SP)], discharging south-eastward into the sea (Figure 1). This bifurcating and branching pattern develops at centennial to millennial time scales, as suggested by a bar migration model (Chen *et al.*, 1985). The mouth zone (coinciding with the maximum turbidity zone) is a morphologically active region where horizontal and vertical circulations play substantial roles in water and sediment transport (Shen *et al.*, 1988; Wu *et al.*, 2010). Tidal currents during flood or ebb peaks are up to 3 m s^{-1}, and strong resuspension causes near-bed suspended sediment concentrations as high as 10 kg m^{-3} (Li and Zhang, 1998; Chen *et al.*, 2006; Liu *et al.*, 2010).

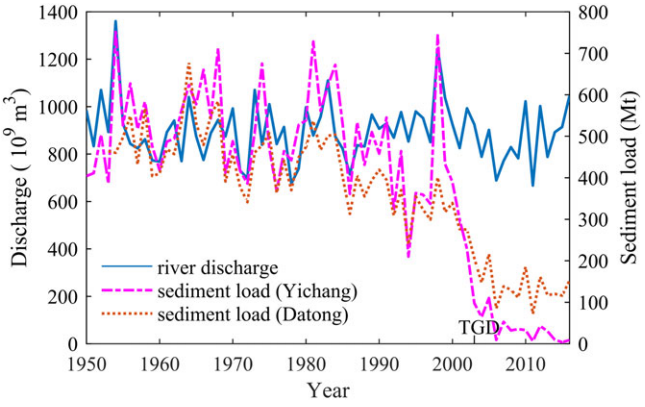

Figure 2. Annual river discharge and suspended sediment load measured at Datong (the most downstream gauging station) and suspended sediment load measured at Yichang (the gauging station immediately downstream of the Three Gorges Dam) between 1950 and 2016. [Colour figure can be viewed at wileyonlinelibrary.com]

The largest local human intervention in the mouth zone is the Deep Channel Navigation Project (DCNP) constructed in the NP (Figure 3a). The elevation of the jetties is approximately 2.0 m above the theoretical lowest water level (TLWL), and the elevation of the groins decreases from 2.0 m at the attachment point to 0 m at the groin head. This elevation suggests that water and sediment are exchanged between the NP and its surrounding shoals only during spring tide high water. The DCNP was constructed between 1998 and 2008, during which time the channel depth was increased from 6 to 9 to 12.5 m. On average, 72 million m^3 of sediment was dredged annually from the NP between 2007 and 2016 (Figure 3). The dredging material was disposed of partly in the shallow areas between the groins and partly offshore (Figure 3a). Some of the sediment disposed between the groins was later transported to the landward part of the Hengsha flat to reclaim land (Figure 3b). Submerged dykes have been built on the landward part of the Hengsha flat, forming an area of ~115 km^2, which has trapped sediment since 2003 (Figure 3a). Moreover, *Spartina alterniflora* and *Phragmites* were artificially introduced to the Jiuduan shoal in 1997 to create a reserve for endangered birds and other species. These measures have significantly influenced the morphological evolution of the mouth zone and are analysed in more detail hereafter.

Data and methods

River discharge and suspended sediment load data were obtained at Datong and Yichang stations from 1950 to 2016 (Changjiang Water Resources Commission, the Ministry of Water Resources of China). Bathymetric data from 1953 to

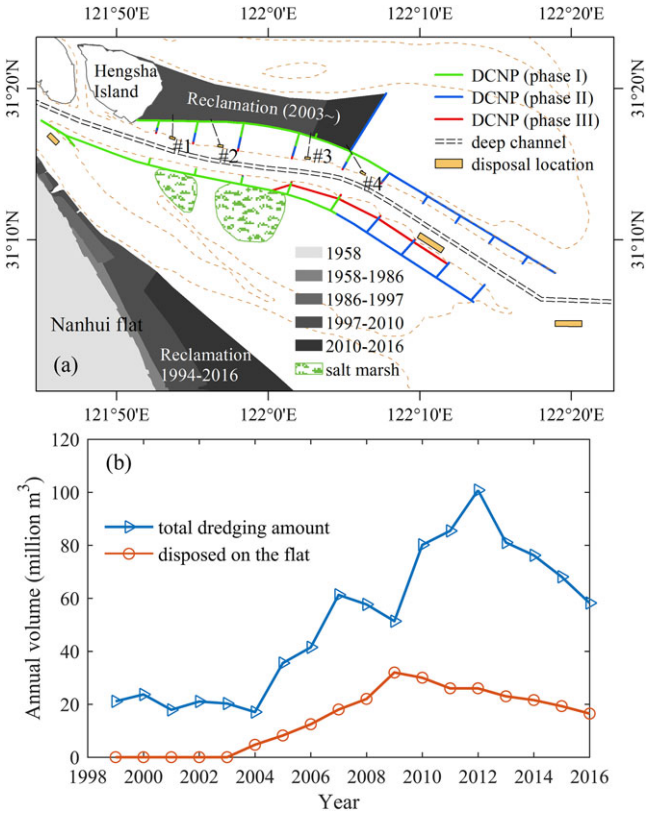

Figure 3. (a) Main human activities in the study area: land reclamation, salt marsh introduction and the DCNP; #1, #2, #3 and #4 are disposal stations where sediment is pumped to the flat. (b) Annual dredging volume and the volume of sediment disposed on the flats in the North Passage. [Colour figure can be viewed at wileyonlinelibrary.com]

1997 were digitized from marine charts, which record historical measurements with an accuracy of ±0.2 m (Table I). The data after 1997 are measured with echo sounders with a vertical accuracy of ±0.1 m. The data accuracy is acceptable for calculation of accretion and erosion volumes on decadal time scales (especially given the relatively large volume changes).

The marine charts were digitized into depth points using the ArcGIS and Surfer software packages. The depth points were interpolated to a digital elevation model (DEM) with a uniform 200 × 200 m grid resolution using kriging techniques. All bathymetric data derived from marine charts and sounding measurements were converted to TLWL (other than for 1953). The difference between the TLWL and the mean water level decreases in the landward direction due to landward decreasing tidal range. All depths used in this study (if not otherwise specified) are positive downward and relative to TLWL.

Bed-level data became unavailable at the Jiuduan shoal (because of vegetation development at bed levels exceeding TLWL) and the landward part of the Hengsha flat (because of land reclamations). To compute volume changes for the complete study area and period, we assumed that (1) the volumes of the Jiuduan shoal above TLWL and (2) the reclaimed region in the landward part of the Hengsha flat did not change after 1997.

We also collected Landsat satellite images of the mouth zone (http://glovis.usgs.gov/) to examine changes in the salt marsh between 1985 and 2016. Salt marshes are mainly present in the supratidal flats and the upper parts of the intertidal flats, whereas the lower parts and the subtidal flats are bare. The interface between bare flats and salt marshes is identified using the normalized difference vegetation index (NDVI) method used in Gao and Zhang (2006) and Li *et al.* (2016). The satellite images are georeferenced and corrected for tidal variations (Table II). Since the salt marsh–bare flat interface is clear and above the water level in all images, the interface is independent of tidal elevations. To sustain data consistency and accuracy, only the images obtained in summer seasons (when vegetation is most evident) are selected. Positive NDVIs indicate intertidal wetlands and marshes occupied by vegetation. To differentiate between vegetation and non-vegetation, a threshold of 0.1 (NDVI $>$ 0.1) is chosen to calculate the vegetated area.

Results

Phenomenological description

In 1953, disconnected flood and ebb channels with slightly different channel alignments developed over a large shoal (Tongsha shoal) in the mouth zone (Figure 4a). The flood and ebb channels were connected in 1958, initiating a new bifurcation and formation of the NP that split Tongsha shoal into the Hengsha flat (the northern part) and the Jiuduan shoal (the southern part) (Figure 4b). The changes between 1953 and 1958 are largely the result of a major river flood occurring in 1954 (with a peak discharge of 92 000 m^3 s^{-1} at Datong), which connected the existing ebb and flood channels (Yun, 2004). Morphologically, the main channels in the mouth zone are very wide and shallow, having width to depth ratios >1000. The sand bars (e.g. the Jiuduan shoal) present large spatial scales with a typical width of ~10 km and length of ~50 km. The wide and shallow features of the YE mouth zone are different from other tide-dominated estuaries (e.g. the Fly Estuary), and the mechanisms responsible for these large dimensions remain poorly known. The morphological evolution of the Hengsha flat and the Jiuduan shoal since 1958 is characterized by fast accretion following their separation. In the period between 1973 and 1986, the northern part of the Hengsha flat grew rapidly (Figures 4d and e). The Jiuduan shoal also grew rapidly after merging with a sand bar from the landward side in 1997 (Figures 4e and f).

The DCNP in the NP significantly disturbed the morphological evolution processes in the mouth zone. The NP narrowed greatly, and its axial alignment was fixed due to the jetties and groins. Lateral water and sediment exchange with adjacent channels were partially blocked, resulting in fast accretion between the groins and over the surrounding flats. Later, the landward part of the Hengsha flat was reclaimed, and the higher part of the Jiuduan shoal (the white area in Figure 4h) became a supratidal flat with limited tidal inundation. Overall, the recent development of the Hengsha flat and the Jiuduan shoal has been strongly influenced by extensive human interference.

Quantitative bathymetric change

The erosion and deposition patterns exhibit strong spatial variations (Figure 5). Erosion and deposition are greatest in the channel–shoal system, reflecting lateral migration of the channels and sand bars. Most net accretion occurs on the Hengsha flat and the Jiuduan shoal. The mouth zone displays erosion and deposition alternating in time. As an example, deposition prevailed east of the Hengsha flat in the periods 1958–1973, 1973–1978 and 1986–1997, whereas erosion dominated in the intervals 1978–1986, 1997–2007, 2007–2010 and 2010–2016 (Figures 5a–g). In the four decades between 1958 and 1997, the Jiuduan shoal accreted continuously. Heavy deposition also occurred in the region to the east of the Hengsha flat and the Jiuduan shoal (approximately along the 10 to 20-m isobaths) (Figure 5h). In contrast, severe erosion was observed there from 1997 to 2016 (Figure 5i). The sheltered regions

Table I. Information about the bathymetric data used in this study

No.	Year	Datum	Sources	Scale	Survey month
1	1953	Approximate lowest low water		1:100 000	—
2	1958			1:25 000	8–10
3	1965			1:100 000	4–11
4	1973				3–11
5	1978		Shanghai Dredging Corporation,	1:50 000	3–7
6	1986		Ministry of Transport of China		5–9
7	1997				12
8	2002				10–11
9	2007			1:25 000	8
10	2010				8
11	2013		The Navigation Guarantee Department		8
12	2016	Lowest normal low water	of the Chinese Navy Headquarters		8

Table II. A summary of the satellite images used in this study. The tidal height references the Wusong datum, which is nearly at the lowest tidal water level. The tidal gauge station Beicaozhong is located in the middle section of the NP

No.	Sensor	Acquisition date	Mapping time (GMT)	Tidal height at Beicaozhong (m)
1	Landsat 5 TM	1989-08-11	01:51:48.2890000Z	2.50
2	Landsat 5 TM	1995-08-12	01:28:34.6590130Z	3.96
3	Landsat 7 ETM +	2000-08-01	02:16:10.7049124Z	3.35
4	Landsat 7 ETM +	2005-08-15	02:14:20.1657199Z	1.91
5	Landsat 5 TM	2009-07-17	02:13:52.5920500Z	2.34
6	Landsat 8 OLI	2013-08-29	02:27:03.2951292Z	2.75
7	Landsat 8 OLI	2016-07-21	02:24:59.1270480Z	3.38

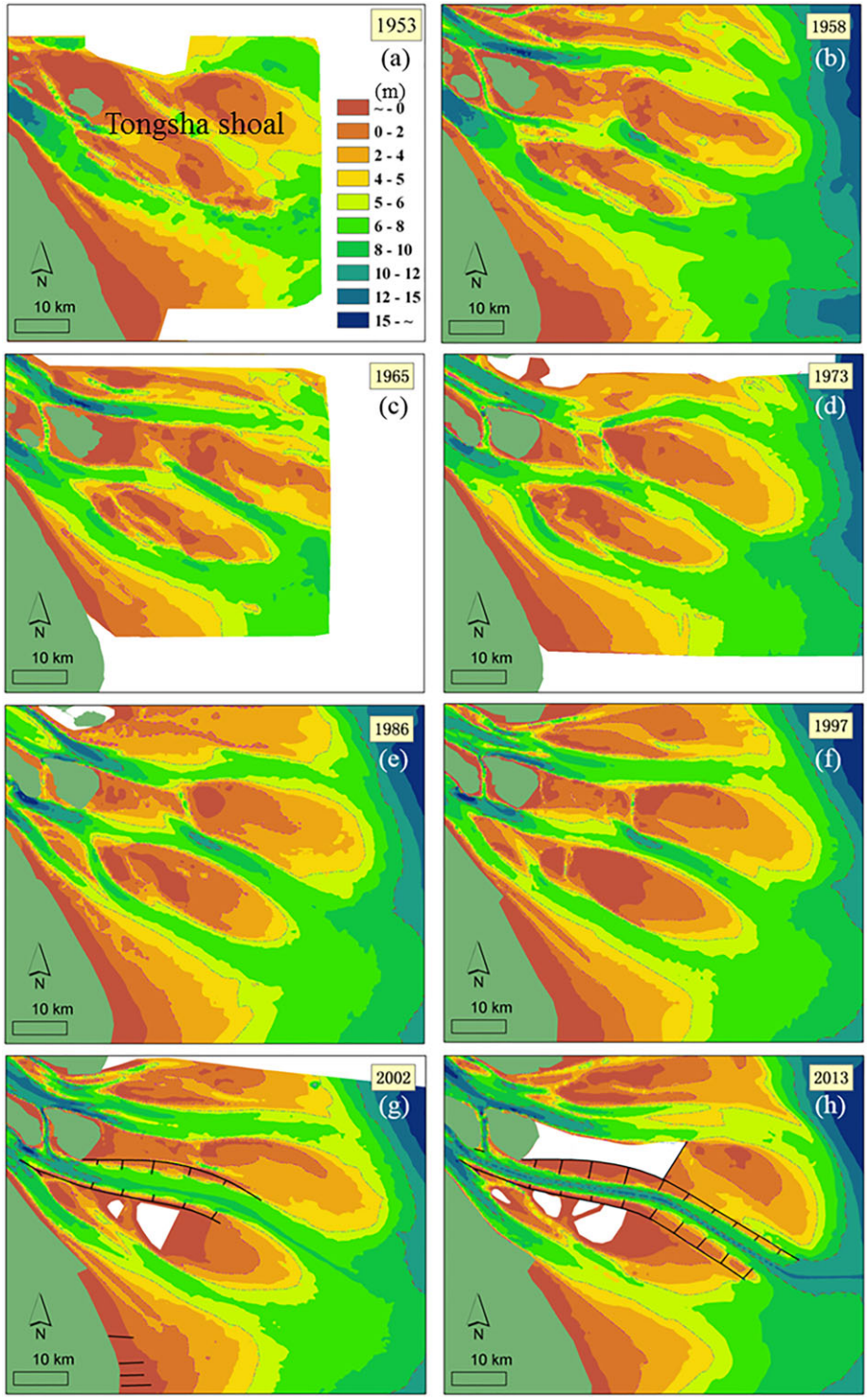

Figure 4. Bathymetric changes of the Jiuduan shoal and the Hengsha flat between 1953 and 2013. [Colour figure can be viewed at wileyonlinelibrary.com]

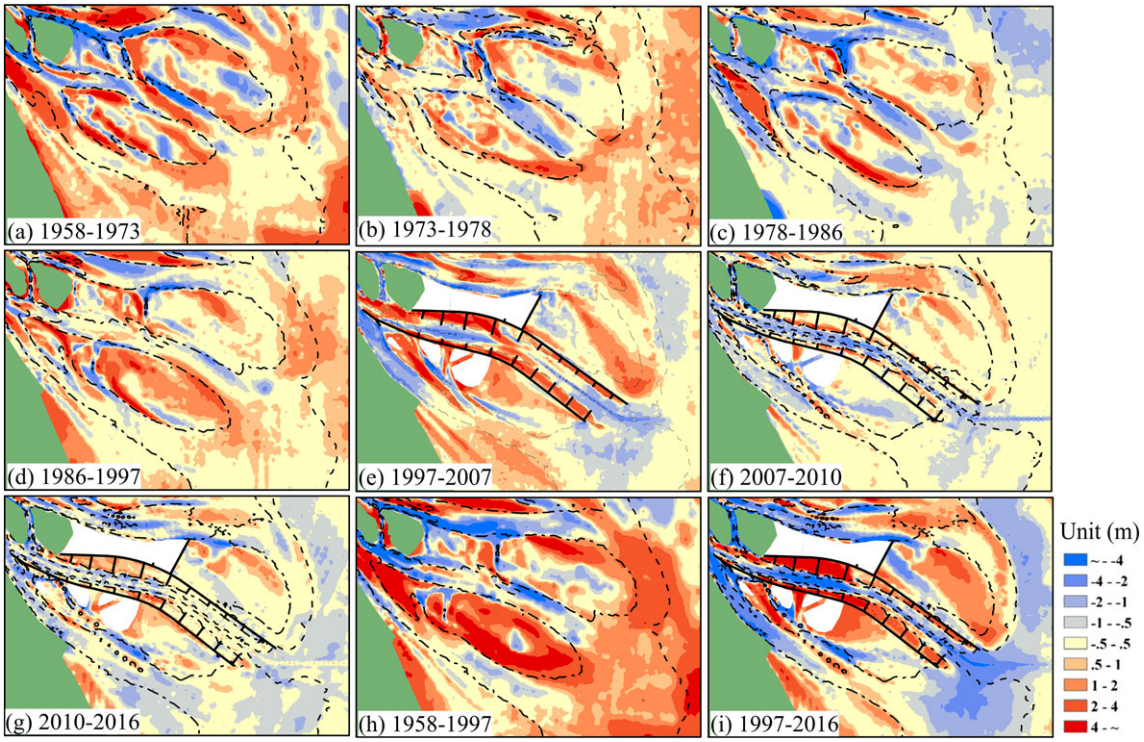

Figure 5. Erosion and deposition patterns [negative bed-level changes (m) indicate erosion and positive values, deposition] in the study area between 1958 and 2016. The 5-m (dot-dashed) and 10-m (dashed) contour lines based on the bathymetry at the end of each period are included for position reference. [Colour figure can be viewed at wileyonlinelibrary.com]

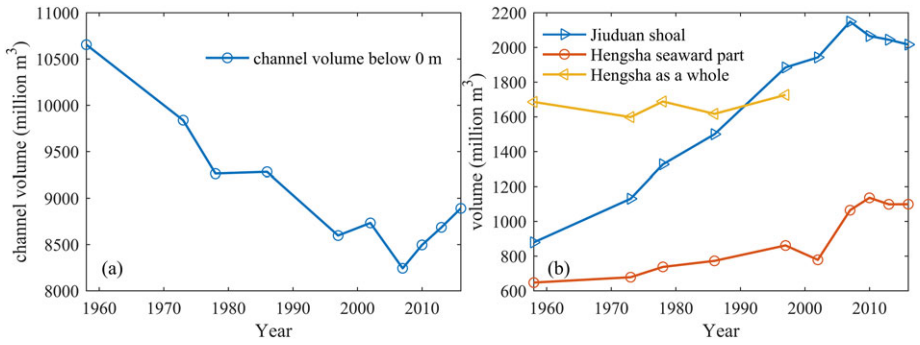

Figure 6. Volume changes of (a) channels below TLWL (in the study area defined in Figure 1) and (b) the Jiuduan shoal and the Hengsha flat (the sediment volume of the area with elevation higher than 6 m below TLWL) between 1958 and 2016. [Colour figure can be viewed at wileyonlinelibrary.com]

between the groins within the NP were rapidly filled from 1997 to 2016 (Figures 5e–g). Deepening along the main waterway was the result of scouring and dredging; their relative importance is evaluated hereafter.

When considering the water volume of the whole study area (Figure 6a), we observe that the water volume below TLWL showed a slight increase between 1997 and 2002 but was followed by an overall decrease from 2002 to 2007. Since 2007, however, the water volume below TLWL has increased, indicating recent erosion of the study area as a whole.

The long-term accretion rates on the Jiuduan shoal are faster than those on the Hengsha flat from 1958 to 2007–2010, followed by erosion until the most recent survey in 2016 (Figure 6b). Specifically, the sediment volume of the Jiuduan shoal (defined as the sand body with a surface depth <6 m, which corresponds approximately to the mean depth of the main channels in the mouth zone), increased continuously by 1269.8 million m^3 between 1958 and 2007 (26 million m^3 $year^{-1}$) and decreased by 132 million m^3 until 2016. The sediment volume of the Hengsha flat did not increase continuously. It decreased slightly between 1958 and 1986, except for a temporary increase between 1973 and 1978. The increase was attributed to deposition of sediment flushed through the North Channel (Yun, 2004). The sediment volume increased slightly (a net volume increase of 109 million m^3) between 1986 and 1997. The sediment volume of the seaward part of the Hengsha flat increased continuously (by 489 million m^3 between 1958 and 2010, except for a decrease from 1997 to 2002), but then decreased by 37 million m^3 between 2010 and 2016. In summary, the volume changes of the channel and the Hengsha flat and Jiuduan shoal indicate a shift from deposition to erosion in approximately 2010.

Hypsometry changes

The morphodynamic evolution of the shoals is analysed in more detail with hypsometric curves, providing areal changes over a continuum of depth classes (Figure 7). The Jiuduan shoal grew fastest at depths below 2 m between 1958 and 1986,

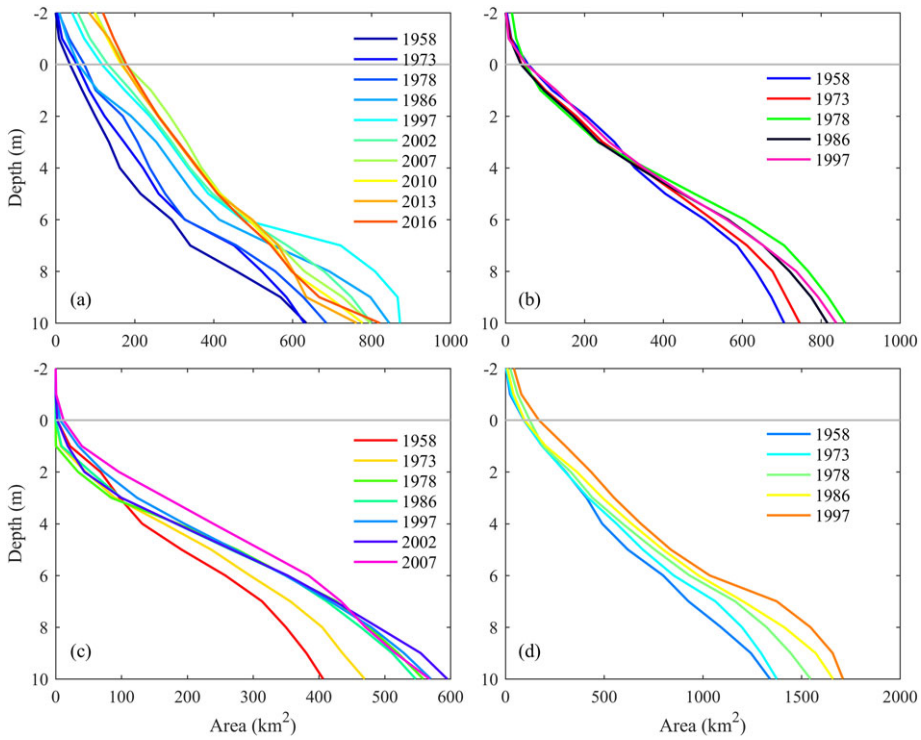

Figure 7. Hypsometry of (a) the Jiuduan shoal, (b) the entire Hengsha flat, (c) the seaward part of the Hengsha flat and (d) the Jiuduan shoal and Hengsha flat. [Colour figure can be viewed at wileyonlinelibrary.com]

followed by rapid accretion at greater depths (>6 m; see Figure 7a). Since 1997, erosion has occurred at depths below 6 m, which is mainly ascribed to deepening of the NP. As a result, the subtidal slope of the Jiuduan shoal became steeper. From 1958 to 1997, the area enclosed by the 6-m isobath increased by 61.5% (from 293.6 to 474.3 km^2). A major increase occurred in the period between 1978 and 1986 due to merging with a sand bar (Figure 8b). Since 1997, the areal growth rate of the flat with a depth smaller than 6 m has decreased, whereas the growth rate of the region with a depth smaller than 0 m continued until 2007 (Figure 8). Therefore, up to 1997, the Jiuduan shoal sustained its profile shape, but after 1997 the profile steepened due to deposition in the upper part and erosion in the lower part.

Because of the partial reclamation of the Hengsha flat, hypsometric curves are provided for the whole flat and for the seaward part only. The hypsometric curves indicate that the shallow parts of the entire Hengsha flat eroded slightly, whereas fast accretion occurred in the deep region between 1958 and 1978. In contrast, the shallow region accreted, whereas the deep region eroded between 1978 and 1997 (Figure 7b). The seaward part of the Hengsha flat developed similarly to the entire Hengsha flat before 1997 and to the Jiuduan shoal after 1997. Specifically, erosion occurred in the regions with depths <3 m (accretion in the deeper zone) during 1958 and 1978, whereas erosion occurred in the regions with depths >8 m (accretion in the shallower zone) between 1997 and 2010 (Figure 7c). The depth at which deposition switches to erosion (or vice versa) was approximately 3–5 m for the Hengsha flat before 1997. For both the Hengsha flat and the Jiuduan shoal, this transitional depth was approximately 8 m from 1997 to 2010. The larger depth threshold is partially explained by the dredging activities in the NP influencing both the Hengsha flat and the Jiuduan shoal. In recent years (2010–2016), the seaward part of the Hengsha flat has been characterized by erosion in the subtidal region at depths >2 m (Figure 7c). The flat area at the 0-m isobath was stable at approximately 50 km^2 before 1997 (Figure 8a). However, the flat area at 6 m increased until 2010, although at a lower rate than the Jiuduan shoal (Figure 8b).

Salt marsh changes

Salt marshes were first observed on the Jiuduan shoal in the late 1980s (Yun, 2004; Shen *et al.*, 2006). *Scirpus mariqueter* was a

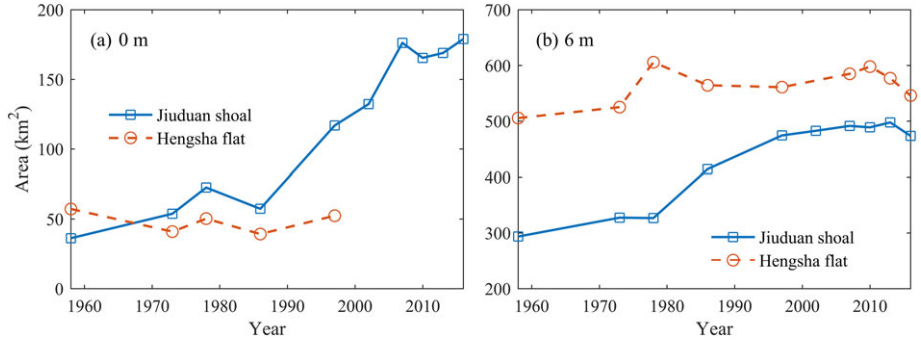

Figure 8. Evolution of the flat area encircled by the (a) 0-m and (b) 6-m isobaths for the Jiuduan shoal and the Hengsha flat between 1958 and 2016. [Colour figure can be viewed at wileyonlinelibrary.com]

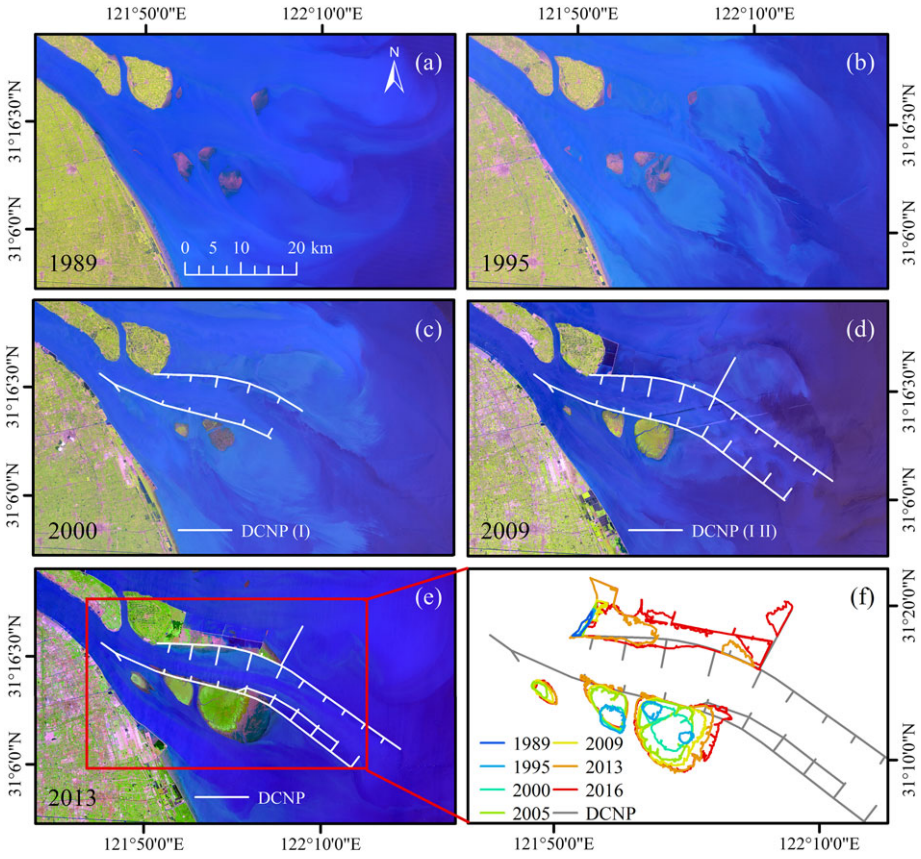

Figure 9. Morphological evolution of the Jiuduan shoal and the Hengsha flat in (a) 1989, (b) 1995, (c) 2000, (d) 2009 and (e) 2013, as recorded by satellite images. (f) Detailed salt marsh boundaries for all years. [Colour figure can be viewed at wileyonlinelibrary.com]

native pioneer species growing in the lower parts of intertidal zones, while a *Phragmites Australis* community dominated the higher parts of the intertidal zone (Li *et al.*, 2016). Plant growth rates increased rapidly after *Spartina alterniflora*, an invasive species, was artificially introduced on the Jiuduan shoal. The salt marsh area increased by 3.0 and 3.9 km^2 $year^{-1}$ in the periods 1995–2000 and 2000–2016, respectively (Figure 9). Most growth (~91%) occurred between 2000 and 2005 (Figure 10). Currently, *Phragmites australis*, *Scirpus mariqueter* and *Spartina alterniflora* are distributed over the Jiuduan shoal, and *Spartina alterniflora* has developed as the dominant species.

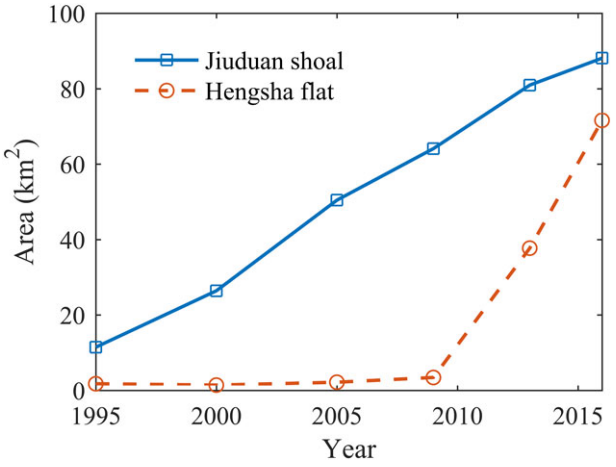

Figure 10. The salt marsh wetland areas of the Jiuduan shoal and the Hengsha flat between 1995 and 2016. [Colour figure can be viewed at wileyonlinelibrary.com]

The Hengsha flat was sparsely vegetated before 2009 (Figures 9 and 10) because of its low elevation. In 2016, the salt marsh area was 71.62 km^2 and was mainly found on the landward part of the Hengsha flat. This growth was the result of the dumping of dredged sediment in the embanked area, sufficiently increasing tidal flat elevation to allow salt marsh growth (Figure 9d). Salt marsh is absent to date in the seaward part of the Hengsha flat because of insufficient elevation.

Overall, the different salt marsh growth patterns and temporal behaviours between the Hengsha flat and the Jiuduan shoal are in line with their morphological evolution patterns (Figure 10). The expansion of salt marshes on the Jiuduan shoal has been continuous since the mid-1990s, whereas salt marshes expanded rapidly on the landward Hengsha flat after 2007.

Discussion

Differences between Hengsha flat and Jiuduan shoal

The morphodynamic evolutions of the Hengsha flat and the Jiuduan shoal are notably different, even though they are geographically close. The Jiuduan shoal accreted at an overall much higher rate than the seaward part of the Hengsha flat in the period from 1958 to 2007–2010. The hypsometric curves of the Jiuduan shoal are more linear, while those of the Hengsha flat are generally S-shaped (see Figure 7). The flat area of the Hengsha flat at the 6-m depth contour increased more than that at 0 m, whereas the flat area of the Jiuduan shoal increased more at the 0-m than at the 6-m isobath (see Figure 8). In other words, the morphodynamic evolution of the Hengsha flat is more prominent in area (horizontal expansion) but less by

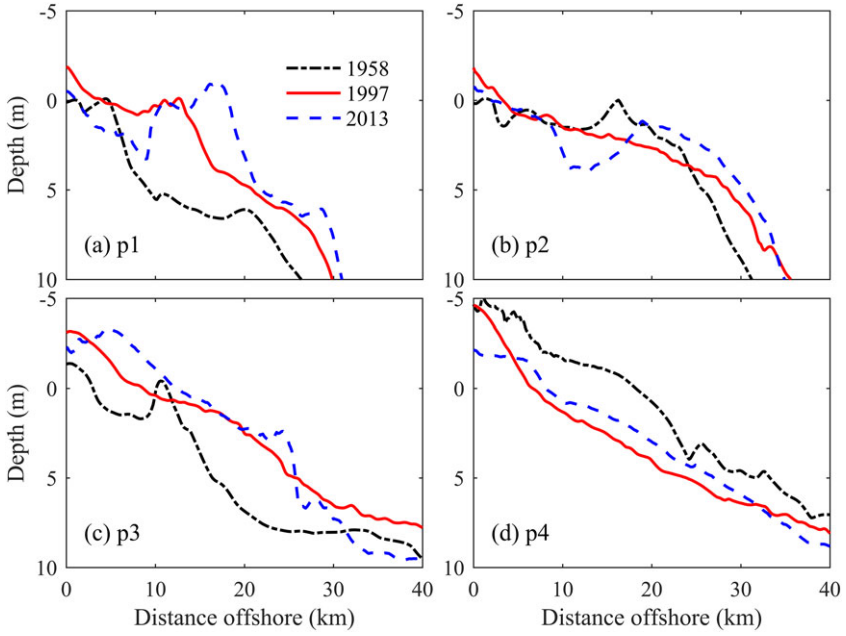

Figure 11. Evolution of the cross-shore profiles to the east of the Hengsha flat and the Jiuduan shoal: (a) p1, (b) p2, (c) p3, (d) p4. The positions of the four profiles are indicated in Figure 1. [Colour figure can be viewed at wileyonlinelibrary.com]

volume (vertical accretion) (see Figures 7 and 8). Similar results were found by Liu *et al.* (2010) and Jiang *et al.* (2012). On its eastern side, the Hengsha flat has a steeper bed slope (i.e. ~1/1200) than the Jiuduan shoal (i.e. <1/4000) (Figure 11). The differences between the two shoals regarding vegetation and the DCNP are discussed later.

We ascribe the differences in the morphodynamic development of the Hengsha flat and the Jiuduan shoal to multiple mechanisms. The shape of the tidal flat is strongly influenced by local hydrodynamics (Kirby, 2000; Le Hir *et al.*, 2000; Roberts *et al.*, 2000). Wave-induced resuspension leads to a landward increase in the sediment concentration. The cross-sectional diffusion of this horizontal concentration gradient by oscillating tidal currents leads to an offshore-directed sediment flux. In the absence of waves, the tidal current favours net sediment transport by settling and scour lags (van Straaten and Kuenen, 1957; Postma, 1961). As a result, a dominance of wave-induced resuspension produces a concave-up profile, whereas a convex-up tidal flat shape is favoured by the dominance of tidal currents (Friedrichs and Aubrey, 1996; Kirby, 2000; Le Hir *et al.*, 2000; Roberts *et al.*, 2000). The Hengsha flat is exposed to stronger north-westerly winds in winter, while the Jiuduan shoal is exposed to weaker south-easterly winds prevailing in summer. As a result, the Hengsha flat should have a more concave-up shape than the Jiuduan shoal (Figure 11). The cross-shore profile shape depends further on the sediment grain size, with muddier sediment tending to generate a more convex profile (Kirby, 2000; Friedrichs, 2011; Zhou *et al.*, 2015). The Jiuduan shoal is muddier than the Hengsha flat (Figure S3), which would further suggest a more convex-up profile. However, the Jiuduan shoal is not convex upwards, particularly in 1958 (Figure 11c). In 1958, the Jiuduan shoal had not yet been merged, so the convex shapes located at 0 and 10 m represent two sand bars (see Figure 4). Since 1997, after the merging of these sand bars, the convex shape of the intertidal zone corresponds to the hydrodynamics and sediment type. The alternating convex and concave shape of the subtidal zone suggests that the profile shape may be influenced by additional factors, likely related to human interventions.

The branching system distributing water and sediment to the various outlets is another factor contributing to the differences. The ebb tidal partition ratio of the North Channel is much larger than those of the SP or NP (Chen *et al.*, 1988). In the past, deposition prevailed in the channel and surrounding flats of a branch that received the largest proportion (>50%) of water and sediment (Yun, 2004). In contrast, erosion occurred in the branch that received less sediment (Dai *et al.*, 2014). The branching dynamics are evidenced by the evolution of the Hengsha flat and the Jiuduan shoal during the late 1970s (see Figure 8). Specifically, the fast accretion of the Hengsha flat in the late 1970s is attributed to deposition of a larger amount of sediment flushed through the North Channel than through the South Channel, while in the meantime the Jiuduan shoal eroded slightly (Yun, 2004). As deposition occurred in the North Channel, the cross-sectional area decreased, leading to a decreasing water volume and sediment supply. This situation provides a negative morphodynamic feedback mechanism, eventually stabilizing the system. Seaward sediment flushing and associated sand bar movements have been observed since 1997 in the North Channel and SP but at much smaller rates, as the channel–shoal pattern has developed towards an equilibrium state (Wang *et al.*, 2013). Similar phenomena are also observed in other tidal estuaries or river deltas with branching channel networks (Sassi *et al.*, 2011; Buschman *et al.*, 2013).

Effect of human intervention

Riverine sediment supply has been decreasing since the mid-1980s, especially in response to the TGD operation since 2003. The Hengsha flat and the Jiuduan shoal sustained accretion until 2007–2010 (Figure 12). A major question therefore is to what extent flat erosion is the result of sediment decline (with a certain time lag) or of local engineering works and/or vegetation changes. Therefore, the various impacts and system responses are summarized in Figure 12.

Effect of sediment decline

Silt and sand are deposited in the TGD reservoir, while most of the clay is flushed seaward. The seaward sediment flux from the Yangtze partly recovers because of along-river erosion between Yichang and Datong (Figure 2; Yang *et al.*, 2011) and downstream of Datong (e.g. the 600-km river reach between Datong and the mouth zone) (Wang *et al.*, 2009; Zhao *et al.*,

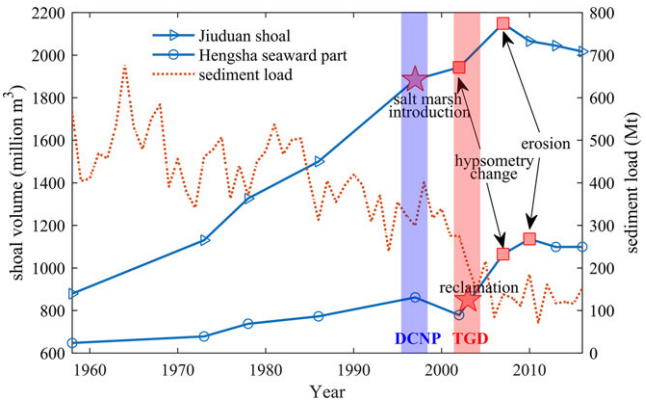

Figure 12. Overview of the evolution of the Hengsha flat and the Jiuduan shoal and changes in suspended sediment load at Datong, with time markers of major human interventions and important morphological changes. The shoal volume refers to the sediment volume of the area with elevation higher than 6 m below TLWL. [Colour figure can be viewed at wileyonlinelibrary.com]

2018). Since the riverbed downstream of Yichang is dominantly sandy, the sand fraction achieves a new equilibrium concentration from bed exchange, whereas the silt fraction does not. The clay fraction is relatively little impacted because it is partly flushed through the reservoirs. Therefore, a reduction in the supply of clay is small; the reduction in silt is large and occurs within a relatively short time period (10–20 years with an assumption of 10% silt content in the riverbed; van Maren *et al.*, 2013), whereas the sand supply has a much longer response time (decades to possibly even centuries, although this estimate is highly speculative at this point).

Erosion has been observed in the subaqueous delta of the YE (e.g. Yang *et al.*, 2011), even though the sediment being deposited there is fine (and therefore not trapped by reservoirs). Even more, the depocenter of the Yangtze subaqueous delta, a mud belt with high sediment exchange, maintains a high deposition rate (Dai *et al.*, 2014). This result suggests that sufficient fine sediment is still supplied from the estuary to maintain the subaqueous delta.

The Hengsha flat and Jiuduan shoal are composed of sand and silt (Figure S3) and therefore respond to suspended sediment load reduction within one to several decades. At present, the sediment concentration appears to have changed little in the study area (Dai *et al.*, 2013; Zhu *et al.*, 2015). However, if the study area reacts to a reduction in the suspended sediment load, such a response would be gradual, leading to a gradual decrease in deposition (possibly followed by a gradual increase in erosion rates). This situation is not observed in the bed-level changes, as discussed hereafter. We further investigate the impacts of human interventions: salt marsh introduction and the DCNP.

Potential impacts of salt marshes

Salt marshes influence morphodynamics by attenuating incoming short waves, trapping fine sediment and stabilizing the bed. All these impacts promote sediment deposition and flat accretion, which is important for coastal restoration and protection. Accretion is further enhanced by the accumulation of biomass in salt marshes (Morris *et al.*, 2002). The introduction of *S. alterniflora* in 1997 most likely facilitated salt marsh growth on the Jiuduan shoal, since *S. alterniflora* expands more rapidly than native species (Huang and Zhang, 2007). The seaward Hengsha flat has only limited vegetation (Figure 9), and as a result the Jiuduan shoal accretes faster than the seaward Hengsha flat.

The impact of the Deep Channel Navigation Project

After the construction of the DCNP started in 1997, severe sedimentation occurred during 2002–2007, following a rapid decrease in accretion. The DCNP can promote accretion by sheltering and sediment-trapping effects induced by deepening. The two jetties along the NP largely reduce horizontal water and sediment circulations among the North Channel, NP and SP in the mouth zone, thereby enhancing accretion of the surrounding flats (Jiang *et al.*, 2012; Li *et al.*, 2016). The embankment of the landward Hengsha flat and the associated dumping there resulted in a rapid increase in the flat elevation. In contrast, deepening may increase the tidal range (Kerner, 2007; van Maren *et al.*, 2015a), salt intrusion (Zhu *et al.*, 2006; Hu and Ding, 2009) and estuarine circulation (Ge *et al.*, 2011; van Maren *et al.*, 2015b), and alter regional hydrodynamics (Jiang *et al.*, 2012) and therefore residual sediment transport. All of these changes are likely to increase sediment concentrations, as found in many estuaries – for example the Ems (Winterwerp *et al.*, 2013; de Jonge *et al.*, 2014), the Elbe (Kerner, 2007; Winterwerp *et al.*, 2013), the Weser (Schrottke *et al.*, 2006) and the Loire (Winterwerp *et al.*, 2013). Additionally, a positive feedback effect between high sediment concentration and tidal amplification further enhances near-bottom sediment trapping (Winterwerp *et al.*, 2009, 2013; van Maren *et al.*, 2015a).

In contrast, the DCNP can affect morphological changes by regulating the diversion ratio of water and sediment discharge through the NP and SP (Jiang *et al.*, 2012). Before construction of the DCNP, the NP discharged more water (~60%) than the SP, but at present the SP discharges ~60% of the water volume (Kuang *et al.*, 2014; Wang *et al.*, 2015). Moreover, the sediment discharged through the NP decreased from ~45% to ~30%, whereas the sediment discharged through the SP increased by 15% from 1998 to 2009 (Kuang *et al.*, 2014). Jiang *et al.* (2012) reported downstream sedimentation in the SP, but erosion can also be expected due to southward dispersion by northerly winds and waves in winter and the longshore current. As a result, the changing water and sediment diversion ratio between the NP and SP influenced erosion and sedimentation in the study area.

Dredging

Dredging volumes along the main waterway in the NP are so large (Figure 3) that they also influence estuarine morphodynamics. Approximately 30% of the dredged sediment has been brought to land since 2003, and this part of the sediment volume needs to be accounted for when interpreting volume changes (Table III and Figure 13). Allowing for some errors, we calculated dredging volumes corresponding to the periods for which chart data are available. When interpreting the bathymetric changes, we define a 'dredging-induced' volume (the volume actually taken out) and a 'natural' volume (the observed changes compensated by dredging volumes). Approximately 35% of the erosion volume in the period 2010–2013 is the result of sediment extraction for land reclamations (dredging-induced). This result highlights the importance of including dredging volumes in the analysis of bed-level changes. In the period 2013–2016, the natural development and bathymetric observations (dashed lines in Figure 13) were depositional again, as they had been before 1997, suggesting time lag effects as discussed later.

It is noted that the dredged and disposed sediment volumes provided here refer to the undisturbed sediment with a dry density estimated as ~1200 kg m^{-3} and not to hopper densities that are more commonly available (see e.g. van Maren *et al.*, 2016). This approach allows a direct comparison of volumes without conversion to sediment mass.

Table III. Volume changes of the study area during different periods

Period	Sediment volume change[a] (million m^3)	Total dredging amount[b] (million m^3)	Sediment disposed to the reclamation area[c] (million m^3)	Equivalent volume disposed to the reclamation area[d] (million m^3)	Net annual sediment deposition/erosion rate[e] (million m^3 $year^{-1}$)	Net annual sediment deposition/erosion rate[f] (million m^3 $year^{-1}$)	Annual sediment load (million ton $year^{-1}$)
1958–1973	824.86	0	0	0	54.99	54.99	478.06
1973–1986	570.17	0	0	0	43.86	43.86	448.00
1986–1997	799.40	0	0	0	72.67	72.67	347.83
1997–2002	2.64	83.72	0	0	0.53	0.53	318.00
2002–2007	942.85	163.88	39.42	47.304	188.57	198.03	177.80
2007–2010	−423.98	187.84	76.50	91.80	−141.33	−110.73	142.50
2010–2013	−267.44	260.6	78.75	94.50	−89.15	−57.65	133.70
2013–2016	116.55	212.68	60.23	72.28	38.85	62.94	126.25
1958–1997	2194.40	0	0	0	56.27	56.27	425.33
1997–2016	370.62	918.36	263.00	315.60	19.51	36.12	159.00
2007–2016	−574.86	659.01	216.00	259.20	−63.87	−35.07	132.00
1958–2016	2565.00	918.36	263.00	315.60	44.22	49.67	273.14

[a]Without disposed sediment on flat (only interpreted from bathymetric maps).
[b]Correspond to Figure 3b.
[c]Correspond to Figure 3b.
[d]Dry density of ~1200 kg m^{-3} for dredged sediment.
[e]Without disposed sediment on flat (only interpreted from bathymetric maps).
[f]With disposed sediment on flat.

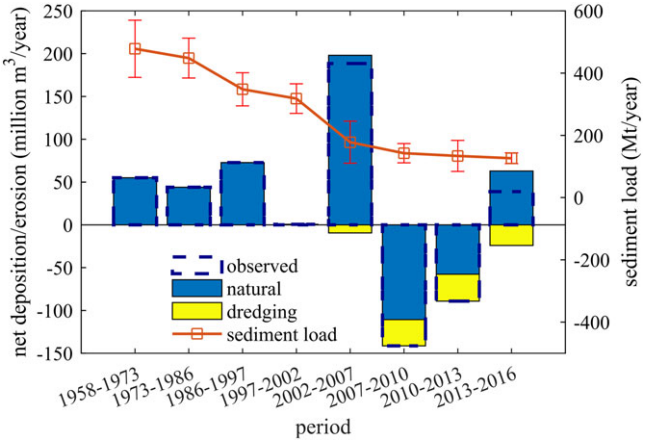

Figure 13. Annual net deposition/erosion of natural development, human-induced development due to dredging and yearly average suspended sediment load changes during different periods. The bars with dashed lines are the volumes quantified by bathymetric data. [Colour figure can be viewed at wileyonlinelibrary.com]

Synthesis

The response of the Yangtze Estuary to human interventions is complicated by time lag effects; the system is so large that time is required for a reduction in sediment supply to take effect. Local engineering works and (human-induced) salt marsh development take place concurrently, probably with much smaller (or even no) time lag effects.

A crucial difference between the impacts of sediment supply and local interventions is the type of system response. A gradual decrease in sediment supply leads to a gradual change in accretion (potentially leading to erosion). A local intervention typically has immediate effects, with a response that gradually decreases with time. Figure 13 reveals a very rapid change from deposition to erosion in approximately 2007; erosion subsequently decreases followed by accretion comparable to that before 1997. This observation strongly supports the interpretation that local interventions were responsible for the major changes that took place in the mouth zone in approximately 2007 and not the reduction in sediment supply (which was also large at approximately this time).

The observation that volume changes were approximately 50 million m^3 from 1958 to 1997 and from 2013 to 2016- (Figure 13) suggests that net volume changes (without local interventions) are fairly constant and not much affected by a reduction in sediment supply. We can simplify the effects of various interventions in the conceptual model depicted in Figure 14 under two assumptions: (1) 'natural' volume changes are fairly constant and approximately 50 million m^3 $year^{-1}$; (2) observed bed-level changes are the result of natural volume changes, dredging and local interventions. In Figure 14, the observed bed levels (based on Figure 13) show rapid fluctuations, whereas the dredging-induced morphological changes are always erosional. As a first step, we compensate the observed bed levels for dredging effects (resulting in the natural, compensated volume change). We can then estimate the effect of local interventions by subtracting this compensated volume change from the natural (assumed) volume change.

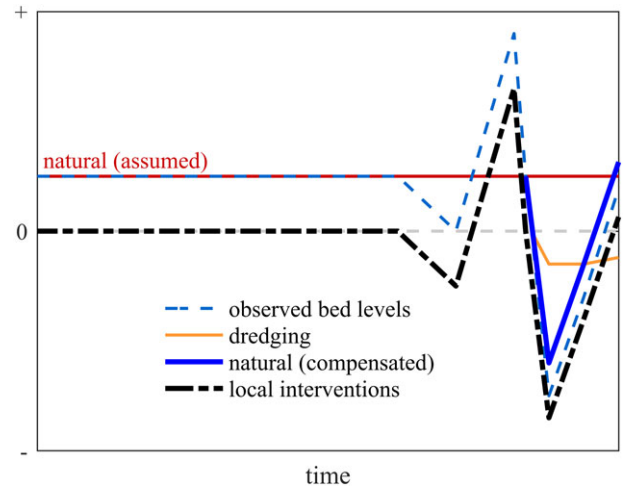

Figure 14. Conceptual model of mouth zone evolution in response to various human interventions according to Figure 13. Positive values indicate deposition, and negative values indicate erosion. [Colour figure can be viewed at wileyonlinelibrary.com]

In general, the effects of local human interventions on an estuary are temporary, leading to local redistribution of sediments; therefore, a new dynamic equilibrium is relatively rapidly attained. Because sediment decline is more permanent in nature, erosion of the estuary mouth lasts much longer (until a new equilibrium between marine erosion and fluvial supply is achieved). Based on our analysis in Figures 13 and 14, it is more likely that the erosion from 2007 to 2013 was temporary and therefore mainly caused by local human interventions. Therefore, we suggest that the morphological adaptation time scale of the mouth zone in response to riverine sediment decline is longer than 30 years (starting from the mid-1980s).

Conclusions

Behaving as a sink of river-supplied sediment, the mouth zone of the YE and its morphological variability are strongly influenced by sediment supply and local human activities. In this study, we use a long time series of bathymetric data and a series of satellite images to examine the 63-year (1953–2016) morphological changes of two large shoals in the YE, the Hengsha flat and the Jiuduan shoal. We conclude that the two shoals sustained accretion until ~2010, followed by erosion. Local human activities are important for morphodynamic changes on the two shoals. The morphodynamic evolution in the pre-1997 period is largely naturally controlled, while the post-1997 evolution is dominantly anthropogenically driven. In particular, from 2002 to 2010 salt marsh introduction and the DCNP stimulated fast accretion of surrounding flats. We also find that the Hengsha flat and the Jiuduan shoal exhibit different morphological behaviours, which can be explained by upstream water and sediment partition, local tidal dynamics and biophysical interactions.

For the whole study area, a sudden shift from accretion to erosion occurred in 2007, mainly in the seaward area of the Hengsha flat and in the Jiuduan shoal. The nearly instantaneous impact is mainly explained by local human interventions. Specifically, the DCNP initially led to heavy sedimentation, followed by years of significant erosion. Further analyses reveal that the disposed volume accounts for up to 35% of the volume changes as quantified by bathymetric data, and therefore needs to be an integral part of the interpretation of erosional and depositional changes. Since the dredging-induced volumes are of the same order as morphologic changes, neglecting them may easily lead to inconsistent conclusions; without considering the effects of dredging and dumping activities, the erosion in the mouth zone may to a large extent be regarded as the effect of reduced sediment supply.

Although future monitoring is still needed to confirm the results, our data suggest a lagging morphological response of the mouth zone in response to the reduction in sediment supply at a time scale of >30 years. Local human interventions play an

important role in masking the gradual effect, and the immediate effect is likely to have been finished in recent years. Our results provide further insight into interpreting morphodynamic changes in large-scale estuaries and deltas under different human activities.

Acknowledgements—This paper is a product of the project 'Coping with deltas in transition' within the Programme of Strategic Scientific Alliances between China and the Netherlands (PSA), financed by the Chinese Ministry of Science and Technology (MOST), Project No. 2016YFE0133700 and the Royal Netherlands Academy of Arts and Sciences (KNAW), Project No. PSA-SA-E-02. This study is also partly supported by the National Natural Science Foundation of China (Nos. 51739005, 51320105005, 41876091), MOST (No. 2017YFE0107400) and the Shanghai Science and Technology Committee (Nos. 17DZ1204800, 18DZ1206400). C. Zhu is supported by the China Scholarship Council (No. 201506140037). Two anonymous reviewers are thanked for their constructive comments and suggestions.

References

Blott SJ, Pye K, van der Wal D, Neal A. 2006. Long-term morphological change and its causes in the Mersey Estuary, NW England. *Geomorphology* **81**: 185–206. https://doi.org/10.1016/j.geomorph.2006.04.008.

Buschman FA, van der Vegt M, Hoitink AJF, Hoekstra P. 2013. Water and suspended sediment division at a stratified tidal junction. *Journal of Geophysical Research: Oceans* **118**: 1459–1472. https://doi.org/10.1002/jgrc.20124.

Chen JY, Zhu HF, Dong YF, Sun JM. 1985. Development of the Changjiang Estuary and its submerged delta. *Continental Shelf Research* **4**: 47–56.

Chen JY, Zhu HF, Dong YF, Sun JM. 1988. Development of the Changjiang Estuary and its subaqueous delta. In *Processes of Dynamics and Geomorphology of the Changjiang Estuary*. Shanghai Scientific and Technical Publishers: Shanghai; 48–62.

Chen SL, Zhang GA, Yang SL, Shi JZ. 2006. Temporal variations of fine suspended sediment concentration in the Changjiang River estuary and adjacent coastal waters, China. *Journal of Hydrology* **331**: 137–145. https://doi.org/10.1016/j.jhydrol.2006.05.013.

Dai ZJ, Chu A, Li WH, Li JF, Wu HL. 2013. Has suspended sediment concentration near the mouth bar of the Yangtze (Changjiang) Estuary been declining in recent years? *Journal of Coastal Research* **29**: 809–818.

Dai ZJ, Liu JT, Wei W, Chen J. 2014. Detection of the Three Gorges Dam influence on the Changjiang (Yangtze River) submerged delta. *Scientific Reports* **4**: 6600. https://doi.org/10.1038/srep06600.

de Jonge VN, Schuttelaars HM, van Beusekom JE, Talke SA, de Swart HE. 2014. The influence of channel deepening on estuarine turbidity levels and dynamics, as exemplified by the Ems estuary. *Estuarine, Coastal and Shelf Science* **139**: 46–59.

De Vriend HJ, Wang ZB, Ysebaert T, Herman PMJ, Ding P. 2011. Eco-morphological problems in the Yangtze Estuary and the western Scheldt. *Wetlands* **31**: 1033–1042. https://doi.org/10.1007/s13157-011-0239-7.

Eidam EF, Nittrouer CA, Ogston AS, DeMaster DJ, Liu JP, Nguyen TT, Nguyen TN. 2017. Dynamic controls on shallow clinoform geometry: Mekong Delta, Vietnam. *Continental Shelf Research* **147**: 165–181. https://doi.org/10.1016/j.csr.2017.06.001.

Fan DD, Wu YJ, Zhang Y, Burr G, Huo M, Li J. 2017. South flank of the Yangtze delta: past, present, and future. *Marine Geology* **392**: 78–93.

Friedrichs C. 2011. Tidal flat morphodynamics: a synthesis. In *Treatise on Estuarine and Coastal Science*, Wolanski E, McLusky D (eds), Vol. **3**. Academic Press: New York; 137–170.

Friedrichs C, Aubrey D. 1996. Uniform bottom shear stress and equilibrium hyposometry of intertidal flats. In *Mixing in Estuaries and Coastal Seas*, Pattiaratchi C (ed). Wiley: New York; 405–429.

Gao A, Yang SL, Li G, Li P, Chen SL. 2010. Long-term morphological evolution of a tidal island as affected by natural factors and human activities, the Yangtze Estuary. *Journal of Coastal Research* **261**: 123–131.

Gao ZG, Zhang LQ. 2006. Multi-seasonal spectral characteristics analysis of coastal salt marsh vegetation in Shanghai, China. *Estuarine Coastal and Shelf Science* **69**: 217–224. https://doi.org/10.1016/j.ecss.2006.04.016.

Ge JZ, Ding PX, Chen CS. 2011. Impacts of Deep Waterway Project on local circulations and salinity in the Changjiang Estuary, China. *Coastal Engineering Proceedings* **1**: 44.

Guo LC, Su N, Zhu CY, He Q. 2018. How have the river discharges and sediment loads changed in the Changjiang River basin downstream of the Three Gorges Dam? *Journal of Hydrology* **560**: 259–274.

Hori K, Saito Y, Zhao QH, Wang PX. 2002. Architecture and evolution of the tide-dominated Changjiang (Yangtze) River delta, China. *Sedimentary Geology* **146**: 249–264. https://doi.org/10.1016/S0037-0738(01)00122-1.

Hu KL, Ding PX. 2009. The effect of deep waterway constructions on hydrodynamics and salinities in Yangtze estuary, China. *Journal of Coastal Research* **S156**: 961–965.

Huang HM, Zhang LQ. 2007. A study of the population dynamics of *Spartina alterniflora* at Jiuduansha shoals, Shanghai, China. *Ecological Engineering* **29**: 164–172.

Jia J, Gao J, Cai T, Li Y, Yang Y, Wang YP, Xia X, Li J, Wang A, Gao S. 2018. Sediment accumulation and retention of the Changjiang (Yangtze River) subaqueous delta and its distal muds over the last century. *Marine Geology* **401**: 2–16. https://doi.org/10.1016/j.margeo.2018.04.005.

Jiang CJ, Li JF, de Swart HE. 2012. Effects of navigational works on morphological changes in the bar area of the Yangtze Estuary. *Geomorphology* **139**: 205–219. https://doi.org/10.1016/j.geomorph.2011.10.020.

Kerner M. 2007. Effects of deepening the Elbe Estuary on sediment regime and water quality. *Estuarine, Coastal and Shelf Science* **75**: 492–500.

Kirby R. 2000. Practical implications of tidal flat shape. *Continental Shelf Research* **20**: 1061–1077.

Kuang CP, Chen W, Gu J, He LL. 2014. Comprehensive analysis on the sediment siltation in the upper reach of the deepwater navigation channel in the Yangtze Estuary. *Journal of Hydrodynamics* **26**(2): 299–308.

Lane A. 2004. Bathymetric evolution of the Mersey Estuary, UK, 1906–1997: causes and effects. *Estuarine Coastal and Shelf Science* **59**: 249–263. https://doi.org/10.1016/j.ecss.2003.09.003.

Le Hir P, Roberts W, Cazaillet O, Christie M, Bassoullet P, Bacher C. 2000. Characterization of intertidal flat hydrodynamics. *Continental Shelf Research* **20**: 1433–1459.

Li JF, Zhang C. 1998. Sediment resuspension and implications for turbidity maximum in the Changjiang Estuary. *Marine Geology* **148**: 117–124. https://doi.org/10.1016/S0025-3227(98)00003-6.

Li X, Liu JP, Tian B. 2016. Evolution of the Jiuduansha wetland and the impact of navigation works in the Yangtze Estuary, China. *Geomorphology* **253**: 328–339. https://doi.org/10.1016/j.geomorph.2015.10.031.

Liu H, He Q, Wang ZB, Weltje GJ, Zhang J. 2010. Dynamics and spatial variability of near-bottom sediment exchange in the Yangtze Estuary, China. *Estuarine Coastal and Shelf Science* **86**: 322–330. https://doi.org/10.1016/j.ecss.2009.04.020.

Luan HL, Ding PX, Wang ZB, Ge JZ, Yang SL. 2016. Decadal morphological evolution of the Yangtze Estuary in response to river input changes and estuarine engineering projects. *Geomorphology* **265**: 12–23. https://doi.org/10.1016/j.geomorph.2016.04.022.

Luo XX, Yang SL, Wang RS, Zhang CY, Li P. 2017. New evidence of Yangtze delta recession after closing of the Three Gorges Dam. *Scientific Reports* **7**: 41735. https://doi.org/10.1038/srep41735.

Morris JT, Sundareshwar P, Nietch CT, Kjerfve B, Cahoon DR. 2002. Responses of coastal wetlands to rising sea level. *Ecology* **83**: 2869–2877.

Postma H. 1961. Transport and accumulation of suspended matter in the Dutch Wadden Sea. *Netherlands Journal of Sea Research* **1**: 148–190.

Roberts W, Le Hir P, Whitehouse R. 2000. Investigation using simple mathematical models of the effect of tidal currents and waves on the profile shape of intertidal mudflats. *Continental Shelf Research* **20**: 1079–1097.

Sassi MG, Hoitink AJF, de Brye B, Vermeulen B, Deleersnijder E. 2011. Tidal impact on the division of river discharge over distributary

channels in the Mahakam Delta. *Ocean Dynamics* **61**: 2211–2228. https://doi.org/10.1007/s10236-011-0473-9.

Schrottke K, Becker M, Bartholomä A, Flemming BW, Hebbeln D. 2006. Fluid mud dynamics in the Weser estuary turbidity zone tracked by high-resolution side-scan sonar and parametric subbottom profiler. *Geo-Marine Letters* **26**: 185–198.

Shen F, Zhou Y, Zhang J, Wu J, Yang S. 2006. Remote-sensing analysis on spatial–temporal variation in vegetation on Jiuduansha wetland. *Oceanologia et Limnologia Sinica* **37**: 504.

Shen HT, Gu GC, Li JF. 1988. Characteristics of the tidal wave propagation and its effect on channel evolution in the Yangtze Estuary. In *Dynamic Process and Geomorphic Development of Changjiang Estuary*, Chen JY, Shen HT, Yun CX (eds). Shanghai Scientific and Technological Press: Shanghai; 73–79 in Chinese.

Sherwood CR, Jay DA, Harvey RB, Hamilton P, Simenstad CA. 1990. Historical changes in the Columbia river estuary. *Progress in Oceanography* **25**: 299–352. https://doi.org/10.1016/0079-6611(90)90011-P.

SOA. 2015. *Bulletin of Chinese sea level rise*. Available at: http://www.coi.gov.cn/gongbao/haipingmian/201603/t20160328_33812.html

Syvitski JPM, Saito Y. 2007. Morphodynamics of deltas under the influence of humans. *Global and Planetary Change* **57**: 261–282. https://doi.org/10.1016/j.gloplacha.2006.12.001.

Thomas CG, Spearman JR, Turnbull MJ. 2002. Historical morphological change in the Mersey Estuary. *Continental Shelf Research* **22**: 1775–1794. https://doi.org/10.1016/S0278-4343(02)00037-7.

van Maren DS, Oost A, Wang Z, Vos P. 2016. The effect of land reclamations and sediment extraction on the suspended sediment concentration in the Ems Estuary. *Marine Geology* **376**: 147–157.

van Maren DS, van Kessel T, Cronin K, Sittoni L. 2015b. The impact of channel deepening and dredging on estuarine sediment concentration. *Continental Shelf Research* **95**: 1–14.

van Maren DS, Winterwerp JC, Vroom J. 2015a. Fine sediment transport into the hyperturbid lower Ems River: the role of channel deepening and sediment-induced drag reduction. *Ocean Dynamics* **65**: 589–605. https://doi.org/10.1007/s10236-015-0821-2.

van Maren DS, Yang SL, He Q. 2013. The impact of silt trapping in large reservoirs on downstream morphology: the Yangtze River. *Ocean Dynamics* **63**: 691–707.

van Straaten L, Kuenen PH. 1957. Accumulation of fine grained sediments in the Dutch Wadden sea. *Geologie en Mijnbouw* **19**: 329–354.

Vörösmarty CJ, Meybeck M, Fekete B, Sharma K, Green P, Syvitski JP. 2003. Anthropogenic sediment retention: major global impact from registered river impoundments. *Global and Planetary Change* **39**: 169–190.

Walling DE. 2009. *The impact of global change on erosion and sediment transport by rivers: current progress and future challenges*. Discussion document for the ISI Workshop, IRTCES, Beijing, November 6.

Wang J, Bai SB, Liu P, Li YY, Gao ZR, Qu GX, Cao GJ. 2009. Channel sedimentation and erosion of the Jiangsu reach of the Yangtze River during the last 44 years. *Earth Surface Processes and Landforms* **34**: 1587–1593.

Wang YH, Dong P, Oguchi T, Chen SL, Shen HT. 2013. Long-term (1842–2006) morphological change and equilibrium state of the Changjiang (Yangtze) Estuary, China. *Continental Shelf Research* **56**: 71–81. https://doi.org/10.1016/j.csr.2013.02.006.

Wang ZB, Van Maren DS, Ding PX, Yang SL, Van Prooijen BC, De Vet PL, Winterwerp JC, De Vriend HJ, Stive MJ, He Q. 2015. Human impacts on morphodynamic thresholds in estuarine systems. *Continental Shelf Research* **111**: 174–183.

Wei W, Dai ZJ, Mei XF, Liu JP, Gao S, Li SS. 2017. Shoal morphodynamics of the Changjiang (Yangtze) estuary: influences from river damming, estuarine hydraulic engineering and reclamation projects. *Marine Geology* **386**: 32–43.

Wei W, Tang ZH, Dai ZJ, Lin YF, Ge ZP, Gao JJ. 2015. Variations in tidal flats of the Changjiang (Yangtze) Estuary during 1950s–2010s: future crisis and policy implication. *Ocean & Coastal Management* **108**: 89–96.

Winterwerp JC, Lely M, He Q. 2009. Sediment-induced buoyancy destruction and drag reduction in estuaries. *Ocean Dynamics* **59**: 781–791.

Winterwerp JC, Wang ZB, van Braeckel A, van Holland G, Kösters F. 2013. Man-induced regime shifts in small estuaries—II: a comparison of rivers. *Ocean Dynamics* **63**: 1293–1306.

Wu H, Zhu JR, Choi BH. 2010. Links between saltwater intrusion and subtidal circulation in the Changjiang Estuary: a model-guided study. *Continental Shelf Research* **30**: 1891–1905. https://doi.org/10.1016/j.csr.2010.09.001.

Yang HF, Yang SL, Meng Y, Xu KH, Luo XX, Wu CS, Shi BW. 2018. Recent coarsening of sediments on the southern Yangtze subaqueous delta front: a response to river damming. *Continental Shelf Research* **155**: 45–51. https://doi.org/10.1016/j.csr.2018.01.012.

Yang SL, Belkin IM, Belkina AI, Zhao QY, Zhu J, Ding P. 2003. Delta response to decline in sediment supply from the Yangtze River: evidence of the recent four decades and expectations for the next half-century. *Estuarine Coastal and Shelf Science* **57**: 689–699. https://doi.org/10.1016/S0272-7714(02)00409-2.

Yang SL, Ding PX, Chen SL. 2001. Changes in progradation rate of the tidal flats at the mouth of the Changjiang (Yangtze) River, China. *Geomorphology* **38**: 167–180. https://doi.org/10.1016/S0169-555x(00)00079-9.

Yang SL, Li H, Ysebaert T, Bouma TJ, Zhang WX, Wang YY, Li P, Li M, Ding PX. 2008. Spatial and temporal variations in sediment grain size in tidal wetlands, Yangtze Delta: on the role of physical and biotic controls. *Estuarine, Coastal and Shelf Science* **77**: 657–671.

Yang SL, Milliman JD, Li P, Xu K. 2011. 50,000 dams later: erosion of the Yangtze River and its delta. *Global and Planetary Change* **75**: 14–20. https://doi.org/10.1016/j.gloplacha.2010.09.006.

Yang SL, Xu KH, Milliman JD, Yang HF, Wu CS. 2015. Decline of Yangtze River water and sediment discharge: impact from natural and anthropogenic changes. *Scientific Reports* **5**: 12581. https://doi.org/10.1038/srep12581.

Yun CX. 2004. *Recent Development of the Changjiang Estuary*. China Ocean Press: Beijing in Chinese with English abstract.

Zhao J, Guo LC, He Q, Wang ZB, van Maren D, Wang XY. 2018. An analysis on half century morphological changes in the Changjiang Estuary: spatial variability under natural processes and human intervention. *Journal of Marine Systems* **181**: 25–36.

Zhou Z, Coco G, van der Wegen M, Gong Z, Zhang C, Townend I. 2015. Modeling sorting dynamics of cohesive and non-cohesive sediments on intertidal flats under the effect of tides and wind waves. *Continental Shelf Research* **104**: 76–91.

Zhu J, Ding P, Zhang L, Wu H, Cao H. 2006. Influence of the deep waterway project on the Changjiang Estuary. In *The Environment in Asia Pacific Harbours*, Wolanski E (ed). Springer: New York; 79–92.

Zhu L, He Q, Shen J. 2018. Modeling lateral circulation and its influence on the along-channel flow in a branched estuary. *Ocean Dynamics* **68**: 177–191.

Zhu L, He Q, Shen J, Wang Y. 2016. The influence of human activities on morphodynamics and alteration of sediment source and sink in the Changjiang Estuary. *Geomorphology* **273**: 52–62. https://doi.org/10.1016/j.geomorph.2016.07.025.

Zhu W, Li J, Sanford LP. 2015. Behavior of suspended sediment in the Changjiang estuary in response to reduction in river sediment supply. *Estuaries and Coasts* **38**: 2185–2197.

Supporting Information

Additional supporting information may be found online in the Supporting Information section at the end of the article.

Table S1. Study periods and study areas in some literatures.

Figure S1. Study area of previous studies (see Table S1) and this study based on bathymetry in 2013.

Figure S2. Bathymetric data points used in this study (scale 1:3,000,000) corresponding to Table 1

Figure S3. Spatial distribution of medium grain size (a), contents of clay (b), silt (c) and sand (d) in bed sediment. Reference position is shown by 5-m (dashed line) contour line. Sum of content of clay, silt and sand is 100%. More details about the data refer to Liu *et al*., (2010).